

Article

# Final Heat Treatment as a Possible Solution for the Improvement of Machinability of Pb-Free Brass Alloys

Anagnostis I. Toulfatzis <sup>1,2</sup>, George A. Pantazopoulos <sup>1,\*</sup> , Constantine N. David <sup>3</sup>,  
Dimitrios S. Sagris <sup>3</sup>  and Alkiviadis S. Paipetis <sup>2,\*</sup>

<sup>1</sup> ELKEME Hellenic Research Centre for Metals S.A., 56th km Athens—Lamia National Road, 32011 Oinofyta, Greece; atoulfatzis@elkeme.vionet.gr

<sup>2</sup> Department of Materials Science and Engineering, University of Ioannina, 45110 Ioannina, Greece

<sup>3</sup> Department of Mechanical Engineering, Technological Education Institute of Central Macedonia, 62124 Serres, Greece; david@teicm.gr (C.N.D.); dsagris@teicm.gr (D.S.S.)

\* Correspondence: gpantaz@elkeme.vionet.gr (G.A.P.); paipetis@cc.uoi.gr (A.S.P.);  
Tel.: +30-2262-60-4463 (G.A.P.); +30-265-100-8001 (A.S.P.)

Received: 4 July 2018; Accepted: 23 July 2018; Published: 25 July 2018



**Abstract:** Heat treatment was performed in order to improve the machinability of three lead-free extruded and drawn brasses, namely CuZn42 (CW510L), CuZn38As (CW511L), and CuZn36 (C27450), based on the concept of microstructural modification. The examined machinability criteria were the following: chip morphology, power consumption, cutting force, and surface roughness. All the above quality characteristics were studied in turning mode in “as received” and “heat treated” conditions for comparison purposes. The selected heat treatment conditions were set for CW510L (775 °C for 60 min), CW511L (850 °C for 120 min), and C27450 (850 °C for 120 min) lead-free brass alloys, according to standard specification and customer requirement criteria. The results are very promising concerning the chip breaking performance, since the heat treatment contributed to the drastic improvement of chip morphology for every studied lead-free brass. Regarding power consumption, heat treatment seems beneficial only for the CW511L brass, where a reduction by 180 W (from 1600 to 1420 W), in relation to the as-received condition, was achieved. Furthermore, heat treatment resulted in a marginal reduction by 10 N and 15 N in cutting forces for CW510L (from 540 to 530 N) and CW511L (from 446 to 431 N), respectively. Finally, surface roughness, expressed in terms of the average roughness value ( $R_a$ ), seems that it is not affected by heat treatment, as it remains almost at the same order of magnitude. On the contrary, there is a significant improvement of maximum height ( $R_t$ ) value of CW511L brass by 14.1  $\mu\text{m}$  (from 40.1 to 26.0  $\mu\text{m}$ ), after heat treatment process performed at 850 °C for 120 min.

**Keywords:** chip morphology; power consumption; cutting force; surface roughness; lead-free brasses; turning; machinability; heat treatment

## 1. Introduction

Leaded brasses are characterized by their great corrosion resistance, electrical conductivity, superior mechanical properties, and formability, but their main industrial use exploits the excellent performance in the machinability, required for high precision and productivity manufacturing processes [1–4]. The mechanical properties and fracture modes under static tensile and impact conditions were studied in the case of conventional leaded brasses (CuZn39Pb3 and CuZn36Pb2As), highlighting the contributing role of  $\beta$ -phase and Pb to failure evolution [5]. Chip fracturing is favoured by the existence of lead particles (Pb content 3 wt. % approximately), which are acting as

a lubricant and facilitate the chip fracturing, minimizing cutting-tool wear [6,7]. Despite the fact that lead presence has many benefits for the machinability, it has also many disadvantages considering the harmful effect of lead in health and environment due to its toxicity. As the requirement for the replacement of leaded brasses by new environmentally friendly brasses (foreseen by the relevant regulations especially for drinking water installations) becomes more explicit, the absence of lead results in poor machinability, restricting quality and productivity of the machining processes [8,9]. Furthermore, from a purely manufacturing-economic standpoint, substitution of lead-containing brass with a lead-free alternative does not appear to be an economically viable option, but it is technically possible, satisfying the requirements of the enforced legislation [10].

Nowadays, the study of machinability of new lead-free brass alloys is of significant interest, although the research in this field is very limited [11–18]. More specifically, fracture properties of lead-free brasses (CW510L, CW511L, C27450) in comparison with a leaded brass (CW614N) was studied in a previous research work, under static and dynamic loading, in order to understand the mechanical behaviour and microstructure relationships for improved machinability [12]. Chip morphology and power consumption corresponding to lead-free brasses versus a conventional leaded brass were studied using Design of Experiment (DOE) technique for the optimization of machinability performance [13]. In a relevant study, chip formation was examined in low- and high- leaded brasses, showing the influence of lead in chip segmentation and the type of chip breakage [14]. Furthermore, in a very recent work, the influence of zinc equivalent on the evaluation of chip morphology and machining surface quality of free cutting silicon brasses was investigated [15]. Also, the influence of tool coating on the workpiece quality, process forces, and chip formation of low-leaded brasses, comparing to a conventional brass was analyzed in turning mode in a similar research [16]. A comparative study of leaded and lead-free brass alloys was implemented concerning the tool wear, cutting force, and surface roughness evaluation during machining in turning mode, showing positive results of substituting the leaded brass for CuZn21Si3P alloy [17]. In a previous work, the Design of Experiments (DOE) technique and Analysis of Variance (ANOVA) were utilized for the optimization of cutting force and surface roughness during machining in turning mode of CuZn42, CuZn38As, and CuZn36 lead-free brasses [18].

According to relevant research, the electrically assisted turning process was employed for the machining of steels (SAE 1020, 1045, 4140) and it has been suggested as a prominent technique, resulting in the improvement of machinability compared with the conventional turning method. Enhancement of surface roughness and reduction of hardness occurred when the turning process is performed using electropulses, especially when lower feed rates are used [19]. In a similar study, the influence of electropulsing on the machinability of steel S235 and aluminium 6060 was studied during conventional and electropulsing-assisted turning processes [20]. The electrically-assisted turning process improved the machinability of steel S235 by decreasing the specific cutting energy, while the machinability of aluminium 6060 was deteriorated by increasing the chip compression ratio. The obtained high values of chip compression ratio signify high strain in the shear plane. Moreover, during turning of aluminium 6060, an increase in cutting speed results in augmentation of chip compression ratio which indicates the occurrence of intense plastic deformation in the chip formation zone.

Heat treatments were also performed to the studied lead-free brass alloys (CuZn42, CuZn38As, and CuZn36), in order to modify the microstructure and increase the  $\beta$ -phase content providing a promising perspective for better chip breakability and improved machinability [21].

The present work is an original contribution pertaining to the optimization of machinability of lead-free brass alloys (CuZn42, CuZn38As, and CuZn36) after heat treatment. The current project possesses a unique advantage, since it aims to improve the machinability of conventional lead-free brass alloys, without altering the material chemistry. This can be also regarded as an attempt to change the metallurgical condition, and, on the other hand, to comply with the product European specification limits, as far as the chemical composition and mechanical properties are concerned. A second, but also significant advantage of this “heat treatment” approach is the avoidance of detrimental hard secondary

phases (such as  $\kappa$ -phase in Si-brasses), which accelerate cutting-tool wear [22]. To the best of our knowledge, no relevant studies have been published concerning the influence of microstructure after heat treatment on the machinability of lead-free brass alloys. In the frame of this work, chip morphology, power consumption, cutting force, and surface roughness were assessed before and after heat treatment to highlight the influence of the modified microstructure on the evolution of machinability quality parameters.

## 2. Materials and Methods

### 2.1. Materials

In this study, extruded and drawn bars with nominal diameter 35 mm and 200 mm length (after hot extrusion and light cold drawing) were selected. These bars originated from three types of lead-free brass alloys (1/2 hard), namely CuZn42 (CW510L), CuZn38As (CW511L), and CuZn36 (C27450). The chemical composition of these brasses was found to be in compliance with EN 12164 standard [23] and Copper Development Association (CDA), as it was determined by optical emission spectrometry (OES) (ARL, Waltham, MA, USA) and X-ray fluorescence (XRF) (ARL, Waltham, MA, USA) and it is depicted in Table 1.

**Table 1.** Chemical composition of the studied brass alloys (expressed in wt. %).

Alloy/(Specification Limits)	Sn	Zn	Pb	Fe	Ni	Al	Cu
CuZn42 (CW510L)	0.0058	Rem	0.10	0.0342	0.0030	0.0002	57.46
EN 12164 (CuZn42/CW510L)	0.30 max	Rem	0.20 max	0.30 max	0.30 max	0.050 max	57–59
CuZn38As (CW511L)	0.0042	Rem	0.09	0.0189	0.0012	0.0002	62.04
EN 12164 (CuZn38As/CW511L)	0.10 max	Rem	0.20 max	0.10 max	0.30 max	0.050 max	61.5–63.5
CuZn36 (C27450)	0.0144	Rem	0.21	0.0244	0.0030	0.0247	63.38
Copper Development Association CDA (CuZn36/C27450)	-	Rem	0.25 max	0.35 max	-	-	60–65

### 2.2. Materials Characterization

Microstructural evaluation was conducted on longitudinal cross-sections after hot mounting, wet grinding, polishing up to 1200 grit paper followed by immersion chemical etching for approximately 5 s at ambient temperature. Immersion etching was performed using a FeCl<sub>3</sub> based solution (8.3 g FeCl<sub>3</sub>-10 mL HCl-90 mL H<sub>2</sub>O), for the alloy CuZn42 (CW510L), while regarding alloys CuZn38As (CW511L) and CuZn36 (C27450), a different solution of FeCl<sub>3</sub> (5 g FeCl<sub>3</sub>-50 mL HCl-100 mL H<sub>2</sub>O) was used according to the ASTM E407-07 standard [24]. Due to the higher percentage of zinc in the case of CuZn42 (CW510L), a different etching solution with lower concentration of HCl was used. Qualitative and quantitative optical metallographic observations were performed using a Nikon Epiphot 300 inverted microscope (Nikon, Tokyo, Japan) assisted by image analysis software (Image Pro Plus, Rockville, MD, USA) for phase (area) fraction determination.

Tensile testing was performed using an Instron 8802, 250 kN (Instron, Norwood, MA, USA) servohydraulic testing machine, at ambient temperature according to BS EN ISO 6892-1 standard [25]. Vickers hardness tests, using a diamond indenter, were performed with an Instron Wolpert 2100 (Instron, Norwood, MA, USA) hardness tester under an 1 kgf (9.807 N) and 0.2 kgf (1.961 N) applied loads, according to the BS EN ISO 6507 standard [26]. Hardness tests were performed at the midway areas of transverse sections ( $\varnothing$ 35 mm), as dictated by EN 12164 standard [23].

### 2.3. Heat Treatment

In a previous work, a series of nine (9) heat treatment schedules was performed. An electrical resistance furnace (Nabertherm GmbH, Lilienthal, Germany) with air circulation and maximum temperature of 850 °C was used for the heat treatment procedure. All the studied brass alloys were

placed in the preheated furnace of 775 °C and 850 °C for 60 min and 120 min, respectively. A rapid water quenching followed at the end of heat treatment.

The optimum heat treatment conditions (temperature, soaking time), which were selected from the nine (9) sets based on EN 12164 specification criteria [21], are the following:

- a. CuZn42 (CW510L): 775 °C for 60 min.
- b. CuZn38As (CW511L): 850 °C for 120 min.
- c. CuZn36 (C27450): 850 °C for 120 min.

The aim of this heat treatment process was the establishment of a microstructure with an augmented  $\beta$ -phase percentage, in order to assist to machinability improvement. This argument is mainly supported by the higher hardness and lower ductility demonstrated by  $\beta$ -phase (bcc-CuZn intermetallic compound), which contributes to the enhancement of chip fragmentation and subsequently to the improved surface roughness and lower cutting forces [27].

#### 2.4. Machinability Testing

Uncoated cemented Mitsubishi carbide cutting-tool inserts, with grade name HTi10, ISO range K10, and ANSI range C3 were used for all the machinability tests. The length of machining, for each bar, was 150 mm and was kept constant throughout the turning process, without lubrication.

Chip morphology was studied by employing a Nikon SMZ 1500 stereo-microscope (Nikon, Tokyo, Japan) and the classification was implemented according to the instructions of ISO 3685 standard [28]. Power consumption was evaluated during the machining by a power meter (PowerLogic PM750, Schneider Electric, Rueil Malmaison, France) connected to the main rotor shaft of the CNC lathe. The machining process executed for evaluation of chip morphology and power consumption was performed in a Computerized Numerical Control (CNC) lathe machine (EMCO PC TURN 155, Hallein-Taxach, Austria).

The main cutting forces were acquired using a 3-axis dynamometer (Kistler 9257B, Winterthur, Switzerland) and an appropriate analog-to-digital device (NI PCI-MIO-16E—1MHz) controlled by means of a graphical user interface (GUI) code developed under LabVIEW 11 software (National Instruments, Austin, TX, USA). A complete system for quantitative 3D Topography including Wyko NT1100 Optical Profiling system (Veeco, Tucson, AZ, USA) supported by Wyko Vision32 analysis, software was utilized for the surface roughness measurements. The three-dimensional roughness average ( $R_a$ ), over the entire measured area, according to ASME-ANSI B46.1 was evaluated [29]. Roughness average values ( $R_a$ ) were selected as the most representative surface topography characteristic, which is commonly used in industrial applications in brass component manufacturing. The evaluation of cutting force and surface roughness measurements was executed in a Computerized Numerical Control (CNC) lathe machine (DMG Alpha 500, DMG MORI CO. LTD, Tokyo, Japan).

In previous research works, machinability tests were performed in turning operation in order to evaluate the chip morphology, the power consumption, the cutting force, and the surface roughness ( $R_a$ ) of CW510L, CW511L, and C27450 lead-free brass alloys, in as-received condition [13,18]. Table 2 shows the combinations of cutting parameters which resulted in the worst result for each specific quality characteristic (chip morphology, power consumption, cutting force, and surface roughness) of the studied lead-free brass alloys, in the “as received” condition. Therefore, the machining parameters which were applied to the heat-treated brasses, were properly selected from Table 2, in order to pursue a direct comparison with the “as received” material condition which exhibited the worst cutting performance, as far as the major quality characteristics were concerned.

**Table 2.** The “worst” combinations of cutting parameters for the quality characteristics (chip morphology, power consumption, cutting force, surface roughness-Ra) of studied lead-free brass alloys in “as received” condition [13,18].

Quality Characteristic	Material	Cutting Speed (rpm)	Depth of Cut (mm)	Feed Rate (mm/min)	Average Value
Chip Morphology (CM)	CW510L	1500	0.5	150	Class. 4 *
	CW511L	2000	1.5	150	Class. 5 *
	C27450	2250	2.0	150	Class. 5 *
Power Consumption (P)	CW510L	1750	1.5	500	1900 W
	CW511L	1750	2.0	250	1600 W
	C27450	2000	1.0	500	1390 W
Cutting Force (CF)	CW510L	1750	1.5	500	540 N
	CW511L	1750	2.0	250	446 N
	C27450	1500	1.5	250	346 N
Surface Roughness (Ra)	CW510L	1750	1.5	500	8.0 $\mu\text{m}$
	CW511L	2250	0.5	500	4.3 $\mu\text{m}$
	C27450	2000	1.0	500	5.6 $\mu\text{m}$

\* Chip Morphology (CM) classification: 1 needle chip, 2 arc chips, 3 conical helical chips, 4 washer-type helical chips, 5 ribbon chips.

### 3. Results and Discussion

#### 3.1. Microstructure and Mechanical Properties

All the studied lead-free brass alloys exhibited a duplex phase microstructure consisting of  $\alpha$  and  $\beta$  phases. Figure 1 depicts representative optical micrographs showing the microstructure of the CuZn42 (CW510L), CuZn38As (CW511L), and CuZn36 (C27450) lead-free brasses in “as received” (Figure 1a–c) and in “heat treated” condition (Figure 1d–f).

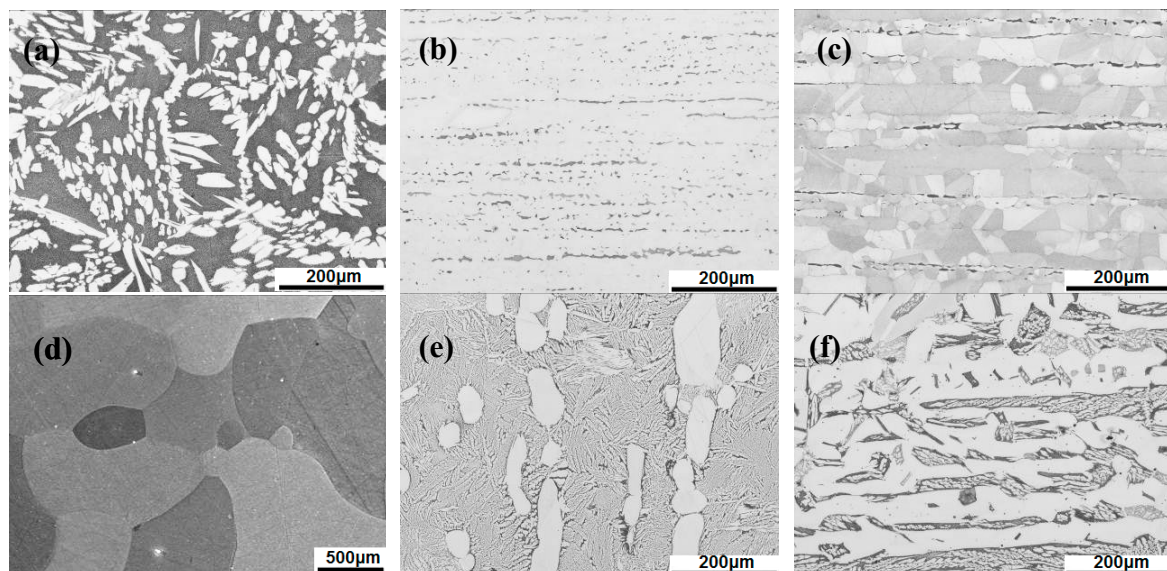


**Figure 1.** Indicative optical micrographs showing the phase structure of longitudinal sections of “as received”: (a) CW510L, (b) CW511L, (c) C27450 and “heat treated” conditions: (d) CW510L, (e) CW511L, (f) C27450 Pb-free brasses. Note that bright areas represent  $\alpha$ -phase and dark areas represent  $\beta$ -phase regions.

Significant changes in phase structure were provoked after heat treatment (Figure 1). More specifically,  $\beta$ -phase content was varied within 20–100% for the examined heat treatment conditions. In the case of CW510L brass, a massive  $\beta$ -phase transformation was achieved, leading to an almost 100%  $\beta$ -phase structure.

In our previous research work, the alteration of microstructure of the lead-free brass alloys due to heat treatment and its influence on mechanical and fracture resistance was thoroughly analyzed [21,30]. More specifically, heat treatment contributed to the increased percentage of  $\beta$ -phase, also seriously modifying the mechanical properties and fracture toughness. The increase of  $\beta$ -phase fraction resulted in alloy strengthening and elongation reduction (as a consequence of grain coarsening and  $\beta$ -phase dominance). The  $\beta$ -phase grain size was varied with respect to temperature and soaking time, as shown in Table 3.

**Table 3.** Average grain size of beta-phase as a function of soaking temperature and duration.

Temperature (°C)	Soaking Time (min)		
	15	60	120
700	Partial beta-phase formation	500–700 $\mu\text{m}$ (~600 $\mu\text{m}$ )	500–700 $\mu\text{m}$ (~600 $\mu\text{m}$ )
775	600–800 $\mu\text{m}$ (~700 $\mu\text{m}$ )	600–800 $\mu\text{m}$ (~700 $\mu\text{m}$ )	600–800 $\mu\text{m}$ (~700 $\mu\text{m}$ )
850	600–800 $\mu\text{m}$ (~700 $\mu\text{m}$ )	1000–1500 $\mu\text{m}$ (~1250 $\mu\text{m}$ )	1000–1500 $\mu\text{m}$ (~1250 $\mu\text{m}$ )

Temperature appeared to be the most significant parameter for grain size control. Machinability tests were subsequently performed for the “optimum” cases of heat treated brasses, where the mechanical properties were found in compliance with the relevant product specifications (Table 4). It was evidenced that the presence of  $\beta$ -phase (especially for CW510L brass alloy) stimulates the occurrence of intergranular fracture, a phenomenon which promotes the easy chip breaking and consequently the lower power consumption. After heat treatment, both CW511L and C27450 alloys, demonstrated fully plastic behaviour, resulting in a completely ductile dimpled fracture. The deeper and coarser dimples, which implied more severe plastic deformation was encountered for the heat treated C27450 brass alloy. Hence, the chip breaking of the two latter brass alloys (CW511L and C27450) is controlled by the maximum allowable plastic strain imposed on the cutting shear zone, which is required for the chip removal.

Characteristic scanning electron microscope (SEM) (FEI, Eindhoven, The Netherlands) micrographs showing the phase structure of the heat treated lead-free brass alloys, under higher magnification, are presented in Figure 2. Except for phase content difference, the variations in phase morphology and distribution were found to be significant, a fact that could potentially affect both the mechanical properties and machinability. In a recently published work, an improvement of fracture toughness was reported for CW510L heat treated brass, in terms of impact energy and Crack-Tip-Opening-Displacement (CTOD) [30].

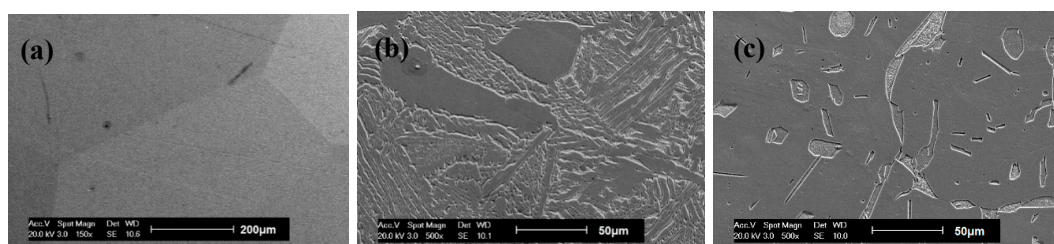


**Figure 2.** Scanning electron microscope (SEM) micrographs of longitudinal sections showing the microstructures of (a) CuZn42 (CW510L), (b) CuZn38As (CW511L), and (c) CuZn36 (C27450), after selected heat treatment conditions.

Microstructure and mechanical properties, after the realization of the optimum heat treatment conditions, are summarized in Table 4, see also the results reported in a previous work [21].

**Table 4.** Phase structure and mechanical characteristics of heat treated lead-free brass alloys.

Brass Alloy	Temperature (°C)	Soaking Time (min)	$\beta$ -Phase (%)	$R_{p0.2}$ (MPa)	$R_m$ (MPa)	$A_{50}$ (%)	$HV_1$ Midway
CW510L	775	60	100	175	430	14	138
CW511L	850	120	35	136	396	44	102
C27450	850	120	20	118	364	47	88

### 3.2. Machinability Evaluation

In previous works, machinability testing was performed in order to evaluate the chip morphology and power consumption, as well as the cutting force and the surface roughness [13,18]. In the previously mentioned studies, machining was conducted in lead-free brass alloys in the “as received” conditions and the optimum cutting parameters were defined by using Design of Experiments (DOE) statistical techniques.

In the present work, the selection of the machining parameters was based on the “worst” case scenario quality results, analyzed in the Section 2.4 (Table 2).

#### 3.2.1. Chip Morphology

The results for the evaluation of chip morphology for each studied lead-free brass after the heat treatment process are depicted in Table 5. Chip morphology was classified according to ISO 3685 [28]. Overall, the turning operation before and after heat treatment resulted in the formation of different chip types from long and continuous chips (washer-type and ribbon) to short and discontinuous chips (arc and conical helical). Similar findings were obtained in a relevant study [31]. Figure 3 presents some of the chips obtained after the machining of the studied brass alloys, under the conditions illustrated in Table 5.

**Table 5.** Chip morphology results of lead-free brasses after the selected heat treatment processes.

Temp. (°C)	Soaking Time (min)	Cutting Parameters			Material	CM (Class.) * As Received	CM (Class.) * Heat Treated
		Cutting Speed (rpm)	Depth of Cut (mm)	Feed Rate (mm/min)			
775	60	1500	0.5	150	CW510L	4	2
850	120	2000	1.5	150	CW511L	5	3
850	120	2250	2.0	150	C27450	5	3

\* Chip Morphology (CM) classification: 1 needle chip, 2 arc chips, 3 conical helical chips, 4 washer-type helical chips, 5 ribbon chips.

The chip morphology for CW510L brass alloy after heat treatment at 775 °C for 60 min, was significantly improved, shifting from “Class. 4” (washer-type helical chips) to “Class. 2” (arc chips). Concerning heat treated CW511L brass alloy (850 °C for 120 min), chip morphology was also substantially improved, as it moved from “Class. 5” (ribbon chips-snarled) to “Class. 3” (conical helical chips). Finally, regarding heat treated C27450 brass alloy (850 °C for 120 min), the chip morphology changed from “Class. 5” (ribbon chips-short) to “Class. 3” (conical helical chips). All the above results are illustrated in Figure 3 and Table 5. As a common observation for all the studied brass alloys, an improvement of chip morphology ranking by two (2) classes after heat treatment was reported. An improved chip breaking capability is directly connected with lower cutting tool wear-rates. The width of the chips varies as a result of the different depth of cut (0.5, 1.50, and 2.0 mm) employed during the various machining experiments. Chip segmentation is of pivotal importance since it facilitates the machining ergonomics and scrap removal without damaging workpiece surface quality and ensuring the safety of the working personnel.

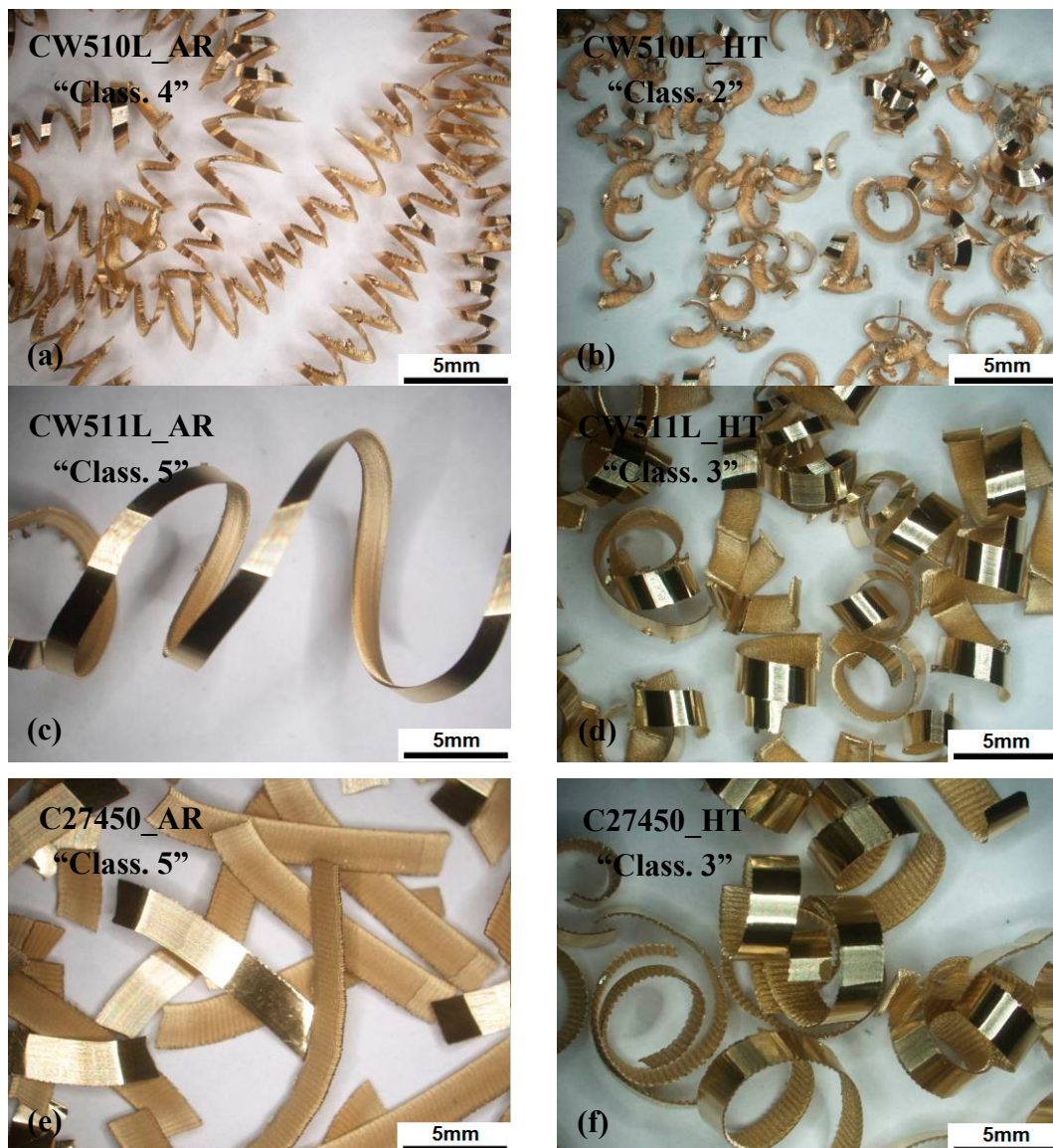


**Figure 3.** Optimum conditions of chip morphology for the studied alloys after heat treatment (“AR”: as received, “HT”: heat treated). (a) CW510L—as received condition, (b) CW510L—heat treated condition, (c) CW511L—as received condition, (d) CW511L—heat treated condition, (e) C27450—as received condition, (f) C27450—heat treated condition.

The highest hardness obtained for CW510L after heat treatment (Table 4) is directly related to a lower percent difference in hardness between the produced chip and the base metal, due to the lower strain hardening rate. This is also related to the lower extent of plastic deformation and hence the ease in chip fracturing and segmentation for the applied machining conditions [13]. Moreover, this argument is also in agreement with the lowest chip morphology obtained in the case of CW510L (Class. 2). The comparison between chip hardness of the as-received and heat treated brass alloys show systematically lower values (by 7–10%), as was anticipated by the limited degree of plastic strain imposed during machining under the final heat treatment condition (Figure 4).

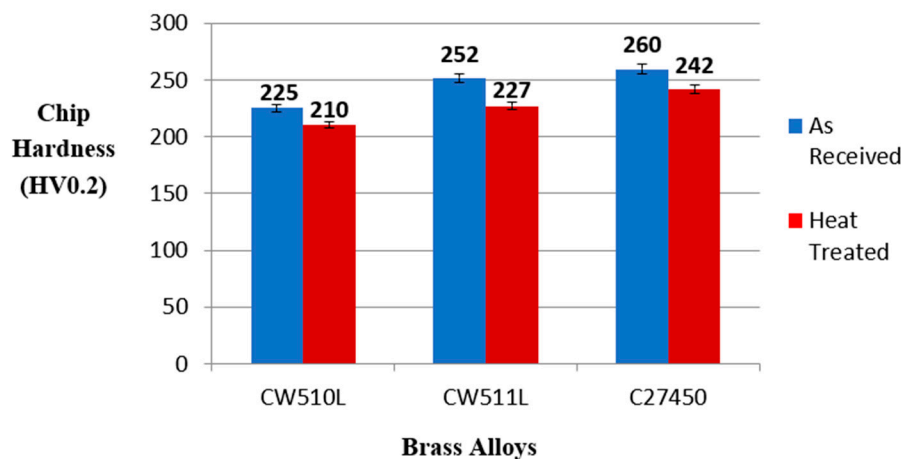


**Figure 4.** Histograms showing the average chip hardness at the “as received” and “heat treated” conditions for the examined brass alloys.

Chip morphologies after heat treatment compared with the as received conditions were studied by optical microscopy for the three lead-free brass alloys (Figure 5). It was observed that heat treatment has a beneficial effect leading to a highest extent of chip segmentation accompanied by a low degree of plastic deformation in the chip/rake face region (Figure 5b,d,f) in relation to as received condition of lead-free alloys (Figure 5a,c,e). Moreover, cracks seem to have evolved at the areas of intense shear band formation, see Figure 5b,d,f. This is in agreement with hardness differences found between chips originating from as-received and heat treated brass alloys, as illustrated in Figure 4.

### 3.2.2. Power Consumption

Heat treatment at 850 °C for 120 min of CW511L lead-free brass alloy yielded a beneficial result with regard to power consumption, where a reduction of 180 W (from 1600 W to 1420 W) compared to the as received condition was observed (Table 6). On the contrary, the power consumption for CW510L and C27450 brass alloys after heat treatment at 775 °C for 60 min and 850 °C for 120 min, respectively, did not show any improvement. More specifically, a moderate increase of 120 W (from 1900 W to 2020 W) and by 70 W (from 1390 W to 1460 W) in CW510L and C27450 brass alloys, respectively, was noticed. All the above results are presented in Table 6. Also, using the present ranking, the highest power consumption was observed in the case of CW510L heat treated brass during turning, as it was also evidenced for the as-received condition. This could be attributed to the fact that the most influential parameter (depth of cut) did not change significantly, especially between the two first classes of brass alloys, i.e., CW510L and CW511L. The hierarchy of cutting process parameters of the three brass alloys (CW510L, CW511L, and C27450), using the Taguchi-DOE technique, was studied and reported in a previous research paper [13].

**Table 6.** Power consumption results of lead-free brasses after the selected heat treatment processes.

Temp. (°C)	Soaking Time (min)	Cutting Parameters			Material	P (W)	
		Cutting Speed (rpm)	Depth of Cut (mm)	Feed Rate (mm/min)		As Received	Heat Treated
775	60	1750	1.5	500	CW510L	1900	2020
850	120	1750	2.0	250	CW511L	1600	1420
850	120	2000	1.0	500	C27450	1390	1460

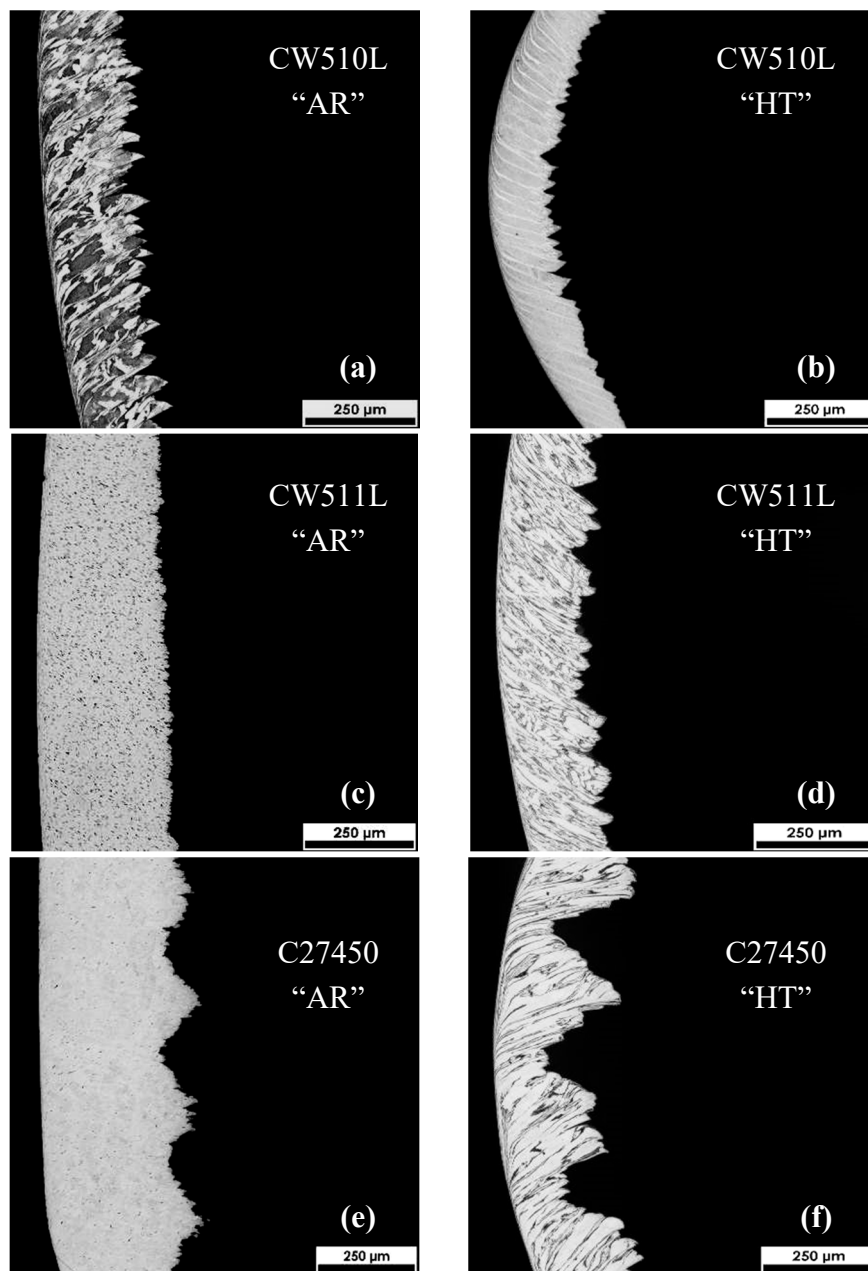


**Figure 5.** Optical micrographs of chip morphologies: (a) CW510L, as received, (b) CW510L, heat treated, (c) CW511L, as received, (d) CW511L, heat treated, (e) C27450, as received, and (f) C27450, heat treated.

### 3.2.3. Cutting Forces

The evolution of cutting force during machining constitutes a common criterion used to evaluate machinability [32]. Cutting force results in the as received and heat-treated conditions are shown in Table 7. More specifically, in CW510L brass, cutting force is improved by 10 N (from 540 to 530 N) after heat treatment at 775 °C for 60 min. In CW511L, there was also a higher reduction of cutting force by 15 N (from 446 to 431 N) after the application of heat treatment at 850 °C for 120 min. Finally, the cutting force was increased by 27 N (from 346 to 373 N), in the case of C27450 brass, after heat treatment at 850 °C for 120 min.

**Table 7.** Cutting force results of lead-free brasses after selected heat treatment processes.

Temp. (°C)	Soaking Time (min)	Cutting Parameters			Material	CF (N)	CF (N)
		Cutting Speed (rpm)	Depth of Cut (mm)	Feed Rate (mm/min)		As Received	Heat Treated
775	60	1750	1.5	500	CW510L	540	530
850	120	1750	2.0	250	CW511L	446	431
850	120	1500	1.5	250	C27450	346	373

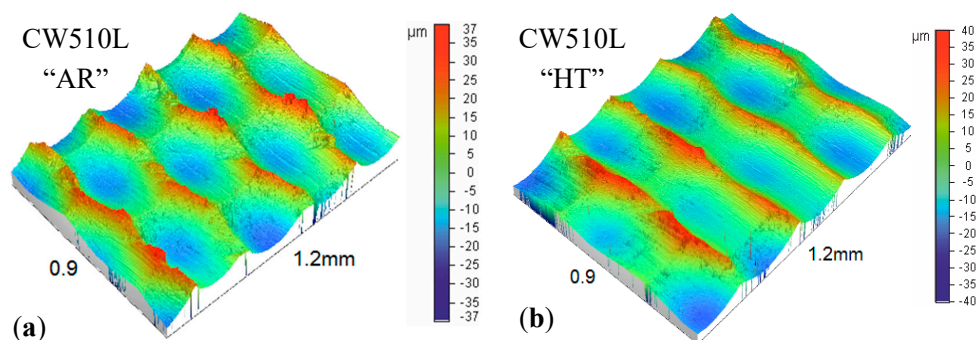
The cutting force results exhibited similar patterns compared with power consumption results (Table 6). Literally, heat treated CW511L brass alloy exhibited the highest reduction in both quality characteristics, while heat treated C27450 showed deterioration in cutting force as well as in power consumption. More specifically, the selected cutting parameters (1750 rpm cutting speed, 2.0 mm depth of cut and 250 mm/min feed rate), contributed to the improvement of cutting force quality characteristic (from 446 to 431 N) for the CW511L brass alloy. The same machining parameters which were used for power consumption measurements (as received vs. heat-treated CW511L alloy) resulted in the improvement of cutting power, from 1600 W to 1420 W. The similar behaviour manifested by the two quality characteristics, i.e., power consumption and cutting force, could be also attributed to their common most influential machining parameter (depth of cut) [18].

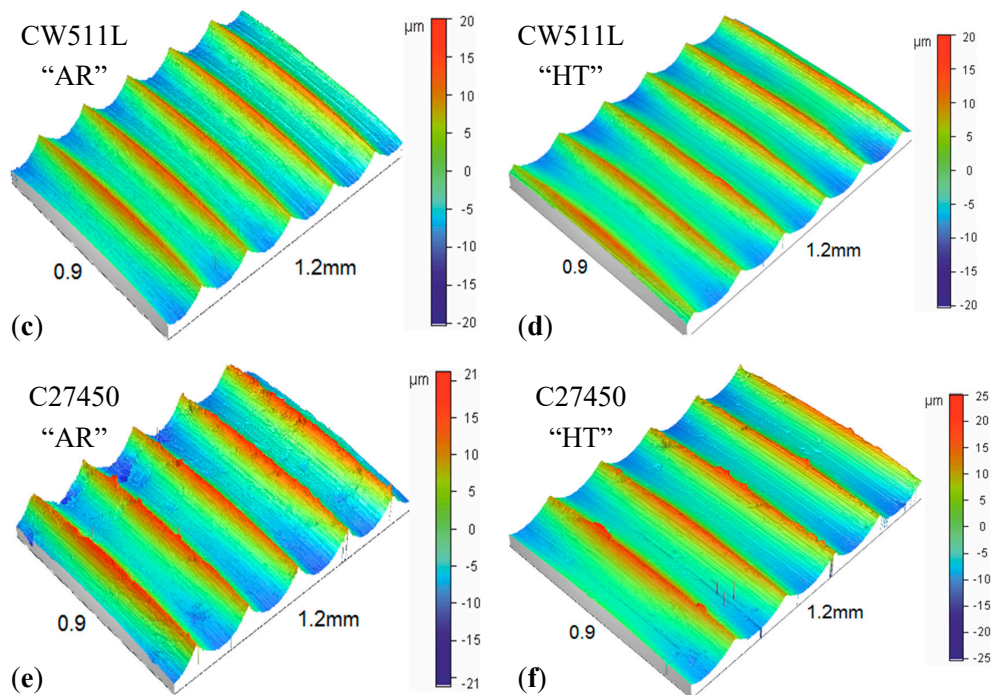
### 3.2.4. Surface Roughness

Figure 6 and Table 8, show the surface roughness and topography results for the studied alloys. It seems that heat treatment in comparison to the as received condition does not show improvement concerning the average roughness value ( $Ra$ ) of the studied brass alloys.

Roughness average ( $Ra$ ) is the primary indicator of surface roughness, but even completely different surfaces can still have the same  $Ra$  value. A surface with sharp spikes, deep pits, or general isotropy may yield the same average roughness value.  $Ra$  makes no distinction between peaks and valleys, nor does it provide information about spatial structure and topography. The surface roughness was also assessed in terms of  $Rt$  parameter to evaluate the surface quality after orthogonal cutting by turning operation [33].  $Rt$  (maximum height—“Peak to Valley”) value is an important indicator of surface roughness which measures the vertical distance between the highest and lowest points in the evaluation length/area.

In this study, it seems that heat treatment of 850 °C at 120 min, although it did not drive to an improvement in  $Ra$  values, it causes a substantial reduction in maximum height ( $Rt$ ) values. This parameter was improved especially in the case of CW511L by 14.1  $\mu\text{m}$  (from 40.1 to 26.0  $\mu\text{m}$ ). Heat treatment at 775 °C for 60 min and 850 °C for 120 min did not show any ameliorated results regarding the  $Rt$  value of CW510L and C27450 lead-free brasses, respectively. More specifically, the  $Rt$  value remained almost the same for CW510L brass (from 78.6 to 79.5  $\mu\text{m}$ ) and it increased for C27450 brass (from 49.2 to 59.4  $\mu\text{m}$ ). All the above results of  $Ra$  and  $Rt$  values are illustrated in Table 8.

**Figure 6.** Cont.



**Figure 6.** Surface topography derived from profilometric measurements: (a) CW510L\_As received, (b) CW510L\_Heat treated, (c) CW511L\_As received, (d) CW511L\_Heat treated, (e) C27450\_As received, and (f) C27450\_Heat treated.

**Table 8.** Surface roughness results of lead-free brasses after selected heat treatment processes.

Temp. (°C)	Soaking Time (min)	Cutting Parameters			Material	SR-Ra (μm)	SR-Ra (μm)	SR-Rt (μm)	SR-Rt (μm)
		Cutting Speed (rpm)	Depth of Cut (mm)	Feed Rate (mm/min)		As Received	Heat Treated	As Received	Heat Treated
775	60	1750	1.5	500	CW510L	8.0	8.5	78.6	79.5
850	120	2250	0.5	500	CW511L	4.3	4.3	40.1	26.0
850	120	2000	1.0	500	C27450	5.6	6.0	49.2	59.4

#### 4. Conclusions

The evaluation of the four quality characteristics i.e., chip morphology, power consumption, cutting forces, and surface roughness, was conducted after heat treatment processes, which were employed as a potential solution for machining performance improvement of lead-free brass alloys (CW510L, CW511L, and C27450). The main findings of this investigation are the following:

- a. The heat treated brass alloys exhibited a significant improvement in chip breaking capability, reducing the chip morphology ranking by two (2) classes:
  - (i) from “Class. 4” (washer-type helical chips) to “Class. 2” (arc chips) for CW510L and
  - (ii) from “Class. 5” (ribbon chips) to “Class. 3” (conical helical chips) for both CW511L and C27450 brass alloys.
- b. Beneficial results in the power consumption were obtained only for the CW511L lead-free brass alloy, showing a reduction by 180 W (from 1600 W to 1420 W) in relation to as received condition. For the CW510L and C27450 lead-free brasses, the heat treatment process did not cause any further improvement.
- c. A slight improvement in cutting forces (approximately by 3%) was recorded in case of heat treated CW511L, which is consistent to the reduction of power consumption results. On the

contrary, an increase in cutting forces (approximately by 8%) was evidenced for the heat treated C27450, as it was also dictated by the power consumption measurements.

- d. Surface roughness measurements, concerning the average roughness ( $R_a$ ) values, seem that they were not affected by the selected heat treatment conditions. Conversely, an appreciable improvement in maximum height ( $R_t$ ) value of the heat treated CW511L brass by 14.1  $\mu\text{m}$  (from 40.1 to 26.0  $\mu\text{m}$ ) was achieved.

As a final note, post-processing heat treatment of Pb-free brass alloys constitutes a promising approach aiming to alter the machinability behaviour through microstructure modification without changing the standard chemical composition and maintaining and even improving the mechanical properties without compromising the plastic behaviour. However, further experimental investigation is necessary to more precisely ascertain the heat treatment conditions and to transfer the process to the industrial scale, in order to design and implement an economically viable manufacturing process with minimum environmental impact.

**Author Contributions:** Conceptualization, A.I.T. and G.A.P.; Investigation, A.I.T., C.N.D. and D.S.S.; Methodology, A.I.T. and D.S.S.; Supervision, G.A.P., C.N.D. and A.S.P.; Writing—original draft, A.I.T.; Writing—review and editing, G.A.P., C.N.D. and A.S.P.

**Funding:** This research received no external funding.

**Acknowledgments:** The authors wish to express special thanks to the Administration and Quality Division of FITCO S.A. for continuous support and providing samples for the current investigation. Special thanks are also addressed to Andreas Rikos and Athanasios Vazdirvanidis (ELKEME S.A.), for their assistance in metallographic sample preparation and examination and for the constructive technical discussion. Finally, special thanks are kindly addressed to Ioannis Evelzaman (Technological Education Institute of Central Macedonia), for his support in CNC machine operation.

**Conflicts of Interest:** The authors declare no conflict of interest.

## References

1. Kuyucak, S.; Sahoo, M. A review of the machinability of copper-base alloys. *Can. Metall. Q.* **1996**, *35*, 1–15. [[CrossRef](#)]
2. Pantazopoulos, G. Leaded brass rods C38500 for automatic machining operations. *J. Mater. Eng. Perform.* **2002**, *11*, 402–407. [[CrossRef](#)]
3. Gane, N. The effect of lead on the friction and machining of brass. *Philos. Mag.* **1981**, *43*, 545–566. [[CrossRef](#)]
4. Garcia, P.; Rivera, S.; Palacios, M.; Belzunce, J. Comparative study of the parameters influencing the machinability of leaded brasses. *Eng. Fail. Anal.* **2010**, *17*, 771–776. [[CrossRef](#)]
5. Pantazopoulos, G.; Toulfatzis, A. Fracture modes and mechanical characteristics of machinable brass rods. *Metallogr. Microstruct. Anal.* **2012**, *1*, 106–114. [[CrossRef](#)]
6. Nobel, C.; Klocke, F.; Lung, D.; Wolf, S. Machinability enhancement of lead-free brass alloys. *Procedia CIRP* **2014**, *14*, 95–100. [[CrossRef](#)]
7. Toulfatzis, A.; Besseris, G.; Pantazopoulos, G.; Stergiou, C. Characterization and comparative machinability investigation of extruded and drawn copper alloys using non-parametric multi-response optimization and orthogonal arrays. *Int. J. Adv. Manuf. Technol.* **2011**, *57*, 811–826. [[CrossRef](#)]
8. Li, S.; Kondoh, K.; Imai, H.; Atsumi, H. Fabrication and properties of lead-free machinable brass with Ti additive by powder metallurgy. *Powder Technol.* **2011**, *205*, 242–249. [[CrossRef](#)]
9. La Fontaine, A.; Keast, V.J. Compositional distributions in classical and lead-free brasses. *Mater. Charact.* **2006**, *57*, 424–429. [[CrossRef](#)]
10. Schultheiss, F.; Windmark, C.; Sjöstrand, S.; Rasmusson, M.; Ståhl, J.E. Machinability and manufacturing cost in low-lead brass. *Int. J. Adv. Manuf. Technol.* **2018**. [[CrossRef](#)]
11. Atsumi, H.; Imai, H.; Li, S.; Kondoh, K.; Kousaka, Y.; Kojima, A. High-strength, lead-free machinable  $\alpha$ - $\beta$  duplex phase brass Cu–40Zn–Cr–Fe–Sn–Bi alloys. *Mater. Sci. Eng. A* **2011**, *529*, 275–281. [[CrossRef](#)]
12. Toulfatzis, A.; Pantazopoulos, G.; Paipetis, A. Fracture behavior and characterization of lead-free brass alloys for machining applications. *J. Mater. Eng. Perform.* **2014**, *23*, 3193–3206. [[CrossRef](#)]

13. Toulfatzis, A.I.; Pantazopoulos, G.A.; Besseris, G.J.; Paipetis, A.S. Machinability evaluation and screening of leaded and lead-free brasses using a non-linear robust multifactorial profiler. *Int. J. Adv. Manuf. Technol.* **2016**, *86*, 3241–3254. [[CrossRef](#)]
14. Nobel, C.; Hofmann, U.; Klocke, F.; Veselovac, D. Experimental investigation of chip formation, flow, and breakage in free orthogonal cutting of copper-zinc alloys. *Int. J. Adv. Manuf. Technol.* **2016**, *84*, 1127–1140. [[CrossRef](#)]
15. Yang, C.; Ding, Z.; Tao, Q.C.; Liang, L.; Ding, Y.F.; Zhang, W.W.; Zhu, Q.L. High-strength and free-cutting silicon brasses designed via the zinc equivalent rule. *Mater. Sci. Eng. A* **2018**, *723*, 296–305. [[CrossRef](#)]
16. Klocke, F.; Nobel, C.; Veselovac, D. Influence of tool coating, tool material, and cutting speed on the machinability of low-leaded brass alloys in turning. *Mater. Manuf. Processes* **2016**, *31*, 895–1903. [[CrossRef](#)]
17. Schultheiss, F.; Johansson, D.; Bushlya, V.; Zhou, J.; Nilsson, K.; Ståhl, J.E. Comparative Study on the Machinability of Lead-Free Brass. *J. Clean. Prod.* **2017**, *149*, 366–377. [[CrossRef](#)]
18. Toulfatzis, A.; Pantazopoulos, G.; David, C.; Sagris, D.; Paipetis, A. Machinability of eco-friendly lead-free brass alloys: Cutting-force and surface-roughness optimization. *Metals* **2018**, *8*, 250. [[CrossRef](#)]
19. Sanchez Egea, A.J.; González Rojas, H.A.; Montilla Montana, C.A.; Kallewaard Echeverri, V. Effect of electroplastic cutting on the manufacturing process and surface properties. *J. Mater. Process. Technol.* **2015**, *222*, 327–334. [[CrossRef](#)]
20. Hameed, S.; González Rojas, H.A.; Perat Benavides, J.I.; Napoles Alberro, A.; Sanchez Egea, A.J. Influence of the regime of electropulsing-assisted machining on the plastic deformation of the layer being cut. *Materials* **2018**, *11*, 886. [[CrossRef](#)] [[PubMed](#)]
21. Toulfatzis, A.; Pantazopoulos, G.; Paipetis, A. Microstructure and properties of lead-free brasses using post-processing heat treatment cycles. *Mater. Sci. Technol.* **2016**, *32*, 1771–1781. [[CrossRef](#)]
22. Taha, M.A.; El-Mahallawy, N.A.; Hammouda, R.M.; Moussa, T.M.; Gheith, M.H. Machinability characteristics of lead free-silicon brass alloys as correlated with microstructure and mechanical properties. *Ain Shams Eng. J.* **2012**, *3*, 383–392. [[CrossRef](#)]
23. European Committee for Standardization (CEN). *BS EN 12164: Copper and Copper Alloys: Rod for Free Machining Purposes*; European Committee for Standardization (CEN): Brussels, Belgium, 2016.
24. American Society for Testing and Materials (ASTM). *ASTM E407-07: Standard Practice for Microetching Metals and Alloys*; American Society for Testing and Materials (ASTM): West Conshohocken, PA, USA, 2007.
25. CEN. *BS EN ISO 6892-1: Metallic Materials—Tensile Testing—Part 1: Method of Test at Room Temperature*; European Committee for Standardization (CEN): Brussels, Belgium, 2009.
26. International Organization for Standardization (ISO). *ISO 6507-1: Metallic Materials—Vickers Hardness Test—Part 1: Test Method*; International Organization for Standardization (ISO): Geneva, Switzerland, 2005.
27. Pantazopoulos, G.; Vazdirvanidis, A. Characterization of microstructural aspects of machinable  $\alpha$ - $\beta$  phase brass. *Microsc. Anal.* **2008**, *22*, 13–16.
28. ISO. *ISO 3685: Tool-Life Testing with Single-Point Turning Tools*; International Organization for Standardization (ISO): Geneva, Switzerland, 1993.
29. ASME. *ANSI B46.1: Surface Texture (Surface Roughness, Waviness, and Lay)*; ASME: New York, NY, USA, 2009.
30. Toulfatzis, A.; Pantazopoulos, G.; Paipetis, A. Fracture mechanics properties and failure mechanisms of environmental-friendly brass alloys under impact, cyclic and monotonic loading conditions. *Eng. Fail. Anal.* **2018**, *90*, 497–517. [[CrossRef](#)]
31. Vilarinho, C.; Davim, J.P.; Soares, D.; Castro, F.; Barbosa, J. Influence of the chemical composition on the machinability of brasses. *J. Mater. Process. Technol.* **2005**, *170*, 441–447. [[CrossRef](#)]
32. Suresh Kumar Reddy, N.; Venkateswara Rao, P. Experimental investigation to study the effect of solid lubricants on cutting forces and surface quality in end milling. *Int. J. Mach. Tools Manuf.* **2006**, *46*, 189–198. [[CrossRef](#)]
33. Zein, H.; Irfan, O.M. Surface roughness investigation and stress modeling by finite element on orthogonal cutting of copper. *Metals* **2018**, *8*, 418. [[CrossRef](#)]

